01,03,12

Magnetic composites based on epoxy resin filled by iron oxide micro- and nanoparticles particles: focus on magnetic detection

© G.Yu. Melnikov, V.N. Lepalovskij, A.P. Safronov, I.V. Beketov, A.V. Bagazeev, D.S. Neznakhin, G.V. Kurlyandskaya

Institute of Electrophysics, Ural Branch, Russian Academy of Sciences, Yekaterinburg, Russia

E-mail: grisha2207@list.ru

Received April 17, 2023
Revised April 17, 2023
Accepted May 11, 2023

Magnetic and structural properties iron oxide micro- and nanoparticles and composites based on epoxy resin at different mass concentrations of particles are investigated (0, 5, 10, 30%). Commercial Alfa Aesar microparticles and nanoparticles obtained by electric explosion of wire with different dispersion parameters were compared. Magnetoimpedance detection of stray magnetic fields of the obtained composites in the form of cylinders using a strip multilayer film element $[FeNi/Cu]_5/Cu/[FeNi/Cu]_5$ was carried out. It is shown that it is possible to determine the position of filled magnetic composites at different mass concentrations of magnetic micro- or nanoparticles with different parameters of dispersion of the ensemble using magnetoimpedance detection

Keywords: magnetic particles, filled magnetic composites, magnetoimpedance effect, multilayer film structures.

DOI: 10.61011/PSS.2023.07.56390.22H

1. Introduction

Magnetic micro- and nanoparticles of iron oxides (MP) — well-studied magnetics, interest into which continues to grow in virtue of their interesting features form the point of view of physics of magnetic materials, technical and biomedical applications [1–3]. Even though most medical applications are oriented at ensembles of magnetic nanoparticles with very narrow distribution by size [2,4], and theoretical calculations are carried out mostly for ensembles of identical superparamagnetic MP [5], in practice production of large batches of such materials is complicated [6]. Besides, if at the level of interaction with a normal cellular membrane or health tissue the requirement of narrow distribution by size is critical, in case of cancer cells or vessels subject to fast growth in process of angiogenesis, there are possible options to use batches with wider distribution of MP by size, since pores of vessels supplying to a tumor may have sizes that are more by an order compared to vessels in the area of healthy tissues [7]. Besides, MP accumulation in biological samples often reflect features of the biological structure. For example, it was found that under certain conditions of interaction of electrostatically stabilized water suspensions based on MP of maghemite with multipotent mesenchymal stromal cells, MP were accumulated in mitochondria in the form of large aggregates [8]. Therefore, the critical objective of biomedical applications is magnetic detection of model aggregates of such formations.

Magnetite particles Fe_3O_4 — available magnetic materials, which may be produced in the form of large batches with various parameters of dispersion by method of electric wire explosion (EWE) [4,9]. On their basis one can produce magnetic composites with various magnetic characteristics due to change in concentration of MP [10,11].

Particles of iron oxide are used in address delivery of medicines, for example, in case of thrombosis, where they are linked to medicine — thrombolytic, and then delivered to the thrombus area, thus developing therapeutically significant local concentration, reducing side effects [12]. You can improve the efficiency of such method with the help of controlling concentration of magnetic particles that deliver thrombolytic to the therapy area (thrombus). MP concentration may be detected with the help o of a detector based on magnetoimpedance effect, thanks to its high sensitivity to external magnetic field. Previously we demonstrated efficiency of detecting a model object in the form of a cylindrical composite based on epoxide resin with commercial microparticles, the average size of which exceeded 200 nm [11]. However, for practical bioapplications requiring delivery in the blood flow, nanoparticles [7] are required, the assessment of the options to detect which will be presented below.

Epoxide resin is one of the important engineering polymer materials, thanks to its strength, good heat and electric insulation properties etc. Based on epoxide resin one may produce composite materials with various fillers by type of nano- and microparticles, which impact the properties of composite [13,14].

Magnetoimpedance (MI) — is a phenomenon of change in ferromagnetic conductor impedance under the action of an external magnetic field when high-frequency current flows in it. Sensitivity up to 300%/Oe [15,16] have been obtained in multilayer film structures. Development of

MI-sensor for detection of particles concentration in case of address delivery requires prior research on model samples with the same magnetic particles. In earlier papers the efficiency of MI-detection of model composites on the basis of epoxide resin with commercial microparticles with very high MP concentration around 30 wt.% [11] was shown. However, data regarding the possibility to detect filled composites with smaller concentrations or nanoparticles as a filler is missing in the literature.

This paper studied structure and magnetic properties of two magnetite MP batches with different features of dispersion, produced by EWE method, and epoxide components on their basis with different MP concentration in the polymer matrix. With the help of rectangular film MI-element $[Fe_{21}Ni_{79}/Cu]_5/Cu/[Fe_{21}Ni_{79}/Cu]_5$ the position of magnetic composites was detected in the form of the cylinder in model geometry simulating thrombus geometry in a blood vessel was detected, and calibration dependence of MI-response on concentration of particles in the composite was built. The comparative analysis of all produced characteristics for composites based on commercial magnetite microparticles was proposed.

2. Measurement techniques and samples

The paper studied three types of particles: A, C, FC. A — commercial microparticles (phases Fe_3O_4 — 94 wt.%, Fe_2O_3 — 1 wt.% and FeO(OH) — 5 wt.%) Alfa Aesar (Ward Hill, MA, USA). Using electrophysical method of EWE, two batches of nanoparticles with different dispersion parameters were produced: C and FC. For bio- and some process applications, the size and possibility to obtain the specified dispersion parameters of the batch are critical parameters that define the possibility to create the device or work under protocol set by governing documents [7]. The electric wire explosion method meets these requirements [9–10].

Based on these three MP batches (A, C and FC), filled magnetic composites were synthesized. They represented epoxide resin with various mass content of particles: 0%, 5%, 10%, 30%. Epoxy-diane resin KDA (Chimex Ltd., Russia) was used as a polymer matrix for the making of composites. First the resin was mixed with hardener — triethylenetetraamine (Epital, Russia) in the ratio of 6 : 1 by weight. Then weighed portions of powders were mixed with a liquid compound of epoxide resit at temperature of 25°C for 10 min. The mixture was then placed in a polyethylene form for hardening during 2 h at 70°C. Magnetic composites had cylinder form with diameter of 5 mm and height of 4 mm. Structural properties were studied using X-ray diffraction analysis (XRDA) and scanning electron microscopy (SEM). In the case of composites, to avoid accumulation of surface charge, a thin conducting film of carbon was applied on the surface of the studied sample by sputtering, and the coating film thickness was around 20 nm. Specific surface was studied using BET method (method of Brunauer–Emmett–Teller). The magnetic properties of the composite were studied using a 7407 VSM vibrating sample magnetometer (Lake Shore Cryotronics, USA) at room temperature. Standard thermomagnet curves of ZFC–FC [9] type were measured in unit SQUID magnetometer MPMS XL7.

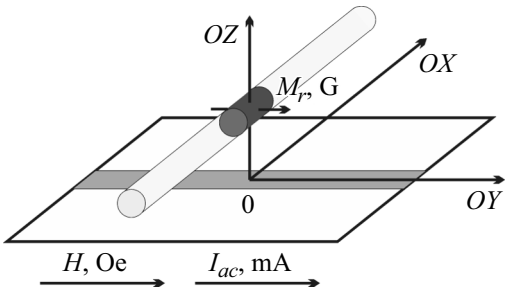

Figure 1. Diagram to detect scattering fields of filled magnetic composites in the form of a cylinder.

It is necessary to explain separately the need of detailed certification of the structure and the magnetic properties of both the MP and the composites on their basis. When certifying nanomaterials, especially oriented at bioapplications, because of manifestration of such phenomenon as polydispersion [7], it is necessary to define one and the same parameter by several independent methods. Thus, in the case of average size of particles, especially for batches with wide distribution by size, they comparatively analyze data of microscopy, XRDA, BET, and also it is possible to use additional magnetic methods. In case of magnetite nanoparticles the analysis of features of Verwey transition [17] using curves ZFC–FC may be very useful to understand the parameters of the structure and size of ensemple particles.

Magnetoimpedance effect of multi-layer film structure $[Fe_{21}Ni_{79}(100\,nm)/Cu(3\,nm)]_5/Cu(500\,nm)/[Fe_{21}Ni_{79}(100\,nm)/Cu(3\,nm)]_5$ (geometric dimensions 10.0×0.5 mm) was measured using the impedance analyzer Agilent HP E 4991 A at room temperature. External magnetic field developed by Helmholtz coils was applied along the longer side of samples (longitudinal magnetic impedance). Range of AC frequencies passing through the element was in the frequency range from 1 MHz to 400 MHz.

MI-response was detected in a configuration which is in demand in bioapplications, namely — for test experiments simulating thrombus passage along a blood vessel. As objects simulating thrombus in a coronary vessel, magnetic composites were selected, the magnetic signal of which was detected with the help of MI-element. Magnetic composite in the form of a cylinder was located at the distance of order 1.10 ± 0.25 mm above the element surface and could move perpendicularly to its long side. Besides, the position of the magnetic composite center varied in respect to the film composite along axis OX (Fig. 1), the pitch was ± 1 mm.

To describe the results of MI-studies used dependence of magnetoimpedance ratio (MI-ratios): $\Delta Z/Z(H) = 100\% \cdot (Z(H) - Z(H_{\max})/Z(H_{\max})$, where $H_{\max} = 100$ Oe — field, where magnetic saturation of the film sample is observed upon application of the external magnetic field along it long side.

Magnetoimpedance response (MI-response) of the element in presence of the scattering fields of the magnetic composite was defined as $\Delta(\Delta Z/Z) = \Delta Z/Z_{control} - \Delta Z/Z_{position}$, where $\Delta Z/Z_{control}$ — MI-ratio measured in presence of a control sample, $\Delta Z/Z_{position}$ — MI-ratio, in the presence of composite in a certain position. Sensitivity to external magnetic field was defined as

$$S = (\Delta Z/Z(H_1) - \Delta Z/Z(H_2)/(H_1 - H_2),$$

where H_1 and H_2 are in the range of linear dependence of MI-ratio on magnetic field.

3. Results and discussion

According to the X-ray diffraction analysis results, the A particles have phase composition: 92% Fe_3O_4, 8% α-FeO(OH). Size of grain defined using Scherrer equation is 240 nm for Fe_3O_4 and 90 nm for α-FeO(OH). Phase composition of C and FC particles is approximately same: 82% Fe_3O_4, 15% Fe_2O_3, 3% α-Fe. Previously it was shown that small quantity of phase α-Fe may be present in magnetite MP produced by EWE method (EWE-MP), as small cores of large particles, which were not oxidized in process of material production. Besides, the main volume of these particles is taken by phase Fe_3O_4 [18]. Phase α-Fe makes a small part, however, its contribution to magnetic properties is significant, i e magnetization of pure iron saturation is much higher than magnetization of saturation Fe_3O_4. Average size of EWE-MP Fe_3O_4 and Fe_2O_3, according to Scherrer equation, approximately corresponds to 150 nm (Fig. 2), even though some features of curve shape near the peak bases indicate possibility of existence of larger quantity of very small MP in the case of FC sample, which is also confirmed by BET data (see below).

One of the features of the crystalline structure of magnetite part is presence of Verwey transition [9,17,18]. Fig. 3 presents dependences of specific magnetic moment on temperature, produced from cooling in zero field (ZFC) and cooling in presence of the field with intensity of 100 Oe (FC). During ZFC process, the sample was heated to temperature 2 K in zero field, then field with intensity of 100 Oe was applied, and the sample was heated to 390 K, and magnetic moment was measured at the same time. FC process was carried out in a similar way, but cooling was carried out in 100 Oe field. ZFC curves of both types of particles (C and FC) have a surge in the area around 100 K, which corresponds to Verwey transition (transition of magnetite from monoclinic syngony to cubic one) for magnetite particles with perfect low-defect

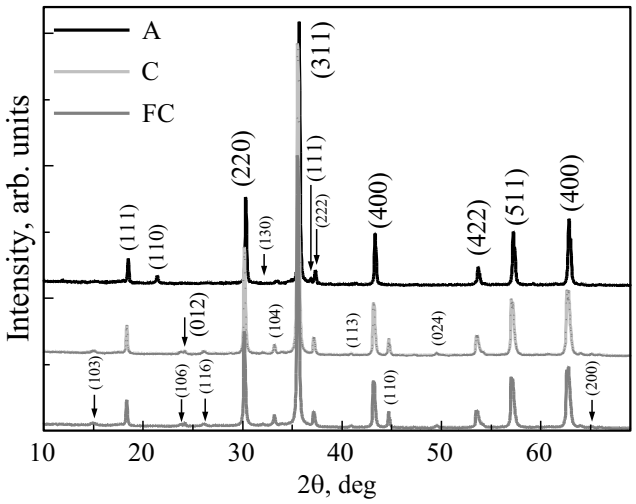

Figure 2. X-ray diffraction analysis of powders A, C and FC. Miller's indices are shown in brackets.

structure at diameter of around 50 nm and more [8,17,18]. When temperature increases to 100 K, ZFC curves have no maximum of magnetic moment, i.e. particles have a wide diversion by parameters.

ZFC and FC curves for particles of type A coincide at temperature over 340 K and spread as it is decreasing. In contrast to particles C and FC, surge at 100 K, corresponding to Verwey transition, is absent (Fig. 3, *a*). This matches XRDA results, indicating certain imperfection of crystal structure of type A particles, even when the average size of commercial microparticles of magnetite is higher than for EWE-MP (table).

Shape and dimensional characteristics of particles of all types were studied using scanning electron microscopy. Size distribution was assessed by SEM photos from a sample consisting of N0 particles. The average diameter of particles was assessed by quantitative distribution of particles $N/N_0 = N/N(d) \cdot 100\%$, where d — particle size, $N(d)$ — number of particles with size d. Quantitative distribution of particles of all types is well approximated by lognormal law, from which one can determine number average diameter of particles d_n (SEM). Weighted average size d_w (SEM) may be assessed using the following equation: $d_w = (\Sigma N_i d_i^4)/(\Sigma N_i d_i^3)$, where N_i means number of particles with certain diameter d_i (table).

According to photographs produced by SEM method, particles of types C and FC have distinct spherical shape, in contrast to particles A, shape of which differs from spherical one, and sometimes there are agglomerates. FC batch is characterized by presence of large particles, around which there are mostly small ones, with average size of $d_n = 20$ nm. Number of large particles is less than small ones, however, their volume fraction is more (Fig. 4).

Another method to assess weighted average diameter is BET method. It helped to determine the value of specific

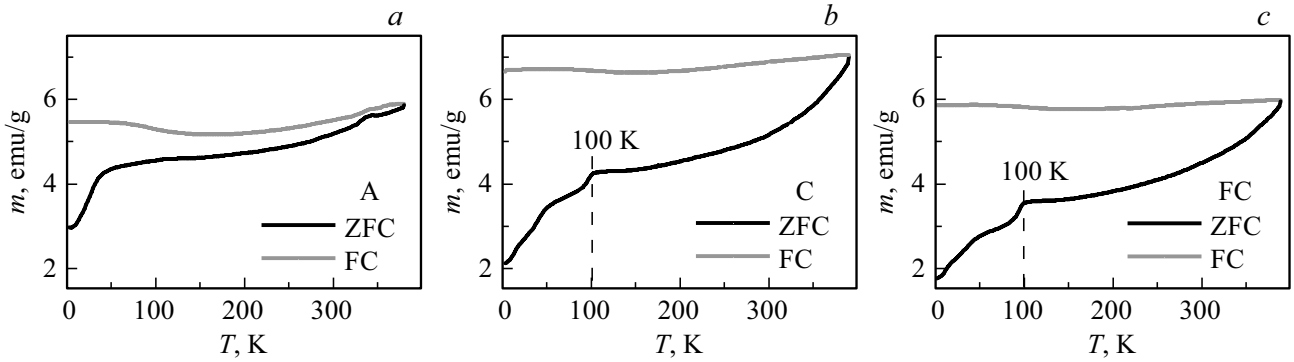

Figure 3. ZFC curves−FC for particles of type: (*a*) A, (*b*) C, (*c*) FC.

Diameter of particles of different types defined by various methods (specified in brackets)

Sample	d_w (XRDA), nm	d_w (SEM), nm	d_n (SEM), nm	d_w (BET), nm
A	240	210	170	167
C	150	230	73	165
FC	150	120	20	46

surface S_{sp} for particles of all types, which makes for particles of type A 6.9 m^2/g, for C — 7.7 m^2/g and for FC — 25.0 m^2/g. The main part of C and FC particles is made up by particles of magnetite (Fe_3O_4) and hematite (Fe_2O_3), density of which is close to $5.2 \cdot 10^6$ g/m^3. Therefore, the weighted average diameter of particles d_w (BET) may be assessed using equation $d_w = 6/(\rho \cdot S_{sp})$.

Weighted average diameter of particles A, determined by SEM method, d_w (SEM) is equal to 210 nm and is close to number average d_n (SEM), equal to 170 nm. By quantitative assessment, the main part of particles C and FC is much smaller A, however, their sample includes large particles. This results in the fact that d_w (SEM) differ greatly from d_n (SEM). Size d_w (BET) of FC and C particles is larger than quantitative dn (SEM), but smaller than weight d_w (SEM) (table). In contrast to size assessment by SEM method using distribution, BET method is sensitive to small particles, which are difficult to identify quantitatively using microscopic methods. On the other hand, even though weight assessments by distribution make it possible to take into account large particles, the quantity of analyzed particles in case of SEM is limited by sample (table).

Structural properties of filled composites were studied by method of scanning election microscopy (Fig. 5). On the photographs the bright points correspond to large particles, which is related to more active interaction of electron beam with oxide particles compared to polymer matrix. Dim points represent small fraction of particles. In contrast to A and C batches, particles of FC type have larger part of small fraction. At small concentrations (5%, fig. 5, *e*) small particles are assembled in aggregates, which are located at a certain distance from each other. When concentration increases to 30%, FC particles fill the composite more evenly (Fig. 5,*f*), compared to, for example, particles of type C (Fig. 5, *d*).

Specific magnetic moment of magnetic particles and composites on their basis was measured at room temperature using VSM. Coercive force H_c values were produced for particles of different types: A — $H_c = 60$ Oe, C — $H_c = 50$ Oe, FC — $H_c = 55$ Oe (Fig. 6, *b*). Coercive force for composite samples does not depend on weight concentration of particles and coincides with coercive force of these particles. (Fig. 6, *c, d*). With growth of concentration the residual specific magnetic moment and specific moment of technical saturation (in field 5 kOe) rises linearly, which means that magnetic properties of particles in composites do not change (Fig. 7). Particles of type C have demonstrated the lowest residual specific magnetic moment ($m_r = 3.1$ emu/g) and the highest specific magnetic moment of technical saturation ($m_s = 82$ emu/g). FC particles, on the contrary, have the highest $m_r = 3.8$ emu/g and the lowest $m_s = 75$ emu/g. Magnetic moment of epoxide resin without nanoparticles is insignificant (Fig. 6, *a*), and it may be neglected. Therefore, such certification of ensembles of magnetic particles produced by various methods or in various conditions, is the basis for understanding features of magnetic detection of model samples produced on their basis.

Magnetoimpedance detection was carried out at current frequency of 127 MHz, since this frequency correlated with the maximum sensitivity to external magnetic field (33%/Oe) in the range of fields from 2 to 5 Oe.

When the magnetic composite gets closer to sensitive element, curves of MI-ratio move to the area of large fields, and maximum value (curve peak) reduces. Such trend is

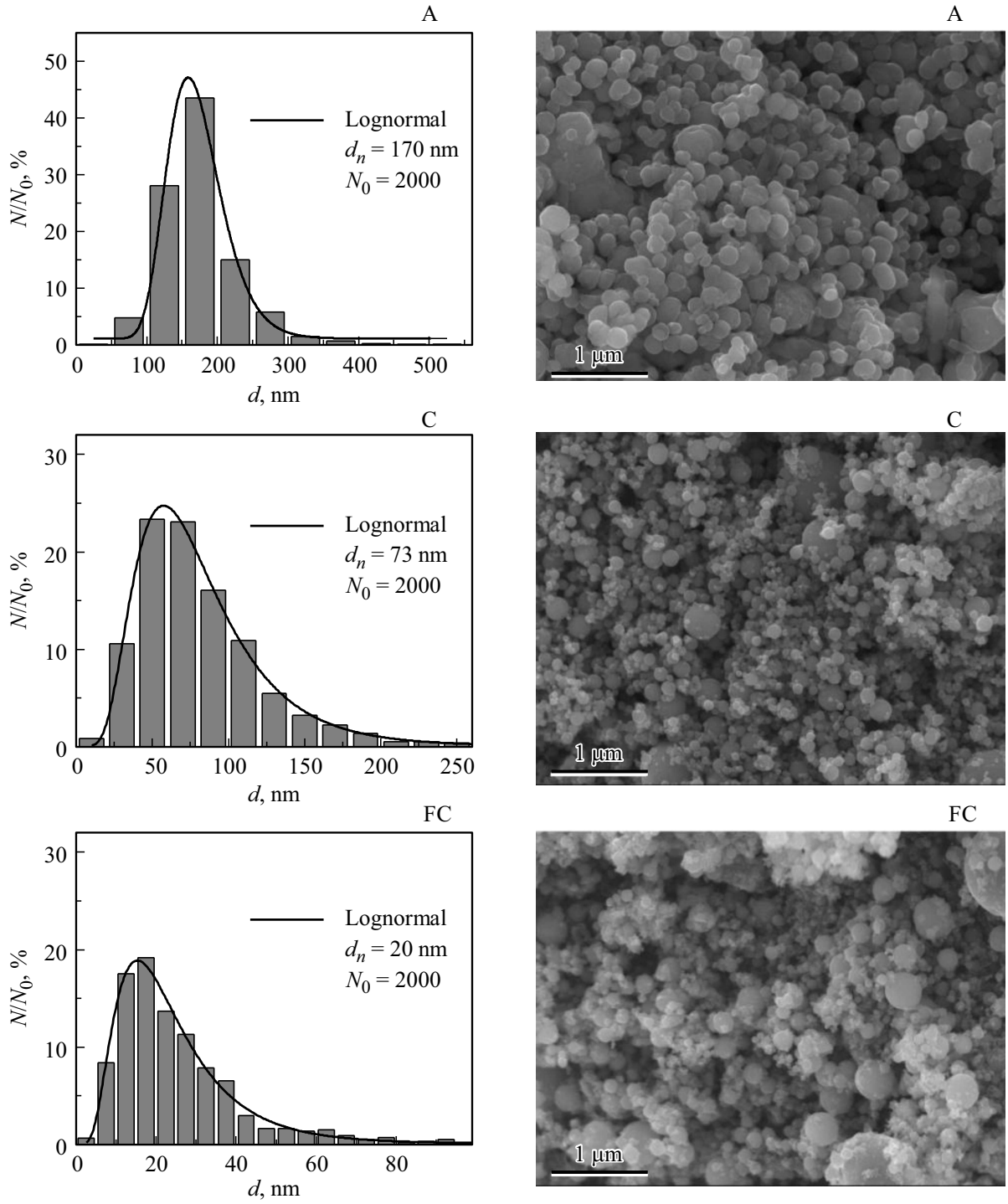

Figure 4. Size distributions and corresponding SEM images for particles of iron oxide A, C, FC.

observed for all composites and matches the results of prior papers [10,19].

As it was shown previously [10], presence of control sample from pure epoxide resin will not impact the MI-ratio of the sensitive element. In this research the control for calculation of MI-response was MI-ratio of the sensitive element (curve „MI“ in fig. 8, *a*). MI-response to composites with the same concentration, but different type of particles is the same. Produced results include experimental errors impacted by several factors. One of them — surface roughness of composites that were not exposed to additional polishing to prevent contamination with magnetic admixtures. Minor heterogeneity is also possible in distribution of filler particles even after thorough preparation of composites with filler in the form of MP ensemble (Fig. 8, *b*). Besides, in these model experiments

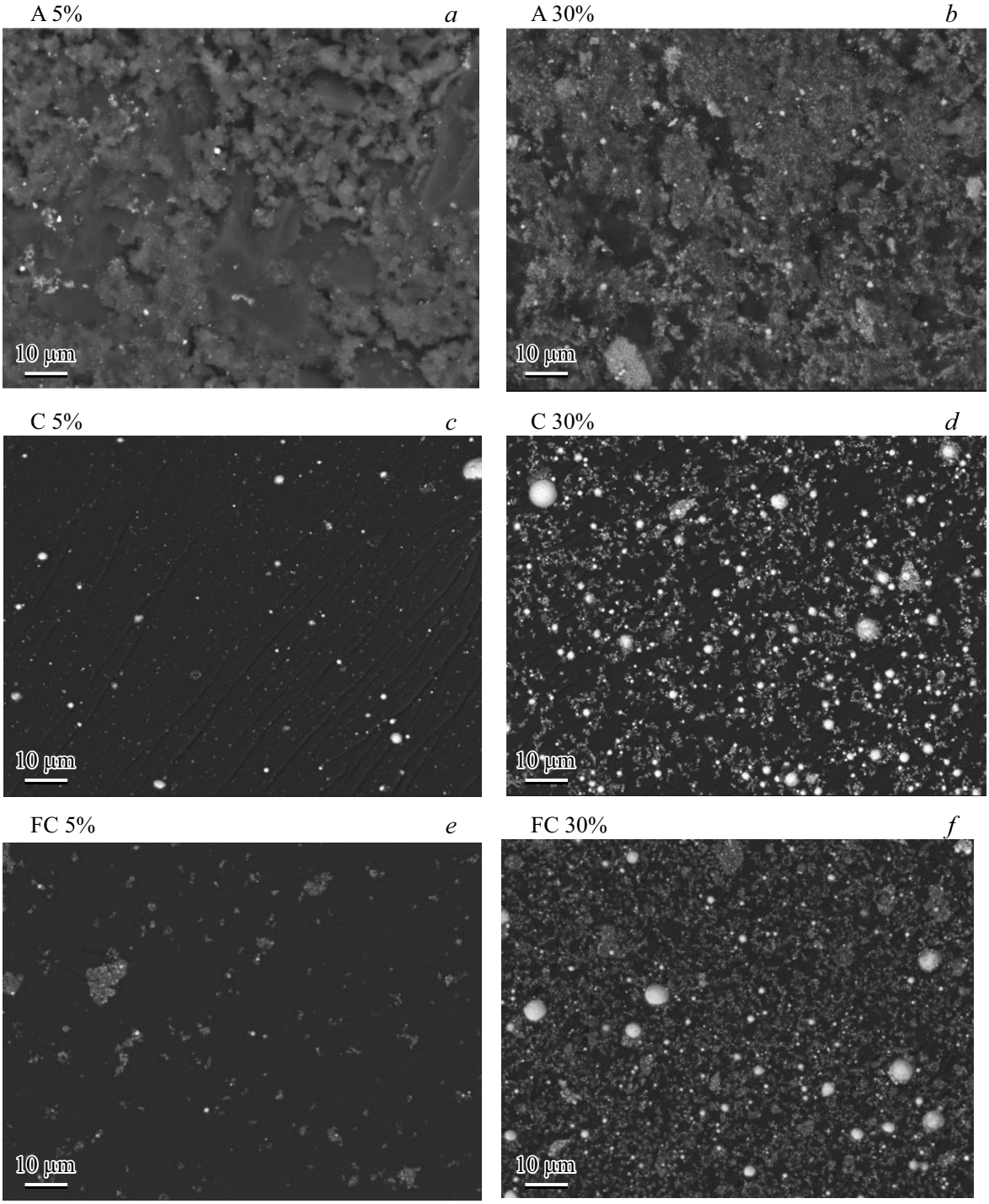

Figure 5. SEM photographs of magnetic composites with weight concentration 5% (a, c, e) and 30% (b, d, f) of magnetic particles of various batches: a, b — A; c, d — C; e, f — FC;

the automatic system of moving the sample in the form of magnetic composite relative to the sensitive element was not used, and the position detection error was at least 0.25 mm. The produced result only reflects the fact that despite significant differences in average sizes and dispersion parameters of used batches of micro- and nanoparticles, when the main magnetic characteristics match, MI-responses in detection of model samples match as well.

Concentration dependences of MI-response in position $OX = 0$ cm, when composites were located above MI-element, are well approximated by linear dependence, which may be used to determine unknown concentration of particles in composites by MI-response (Fig. 8, c). Based

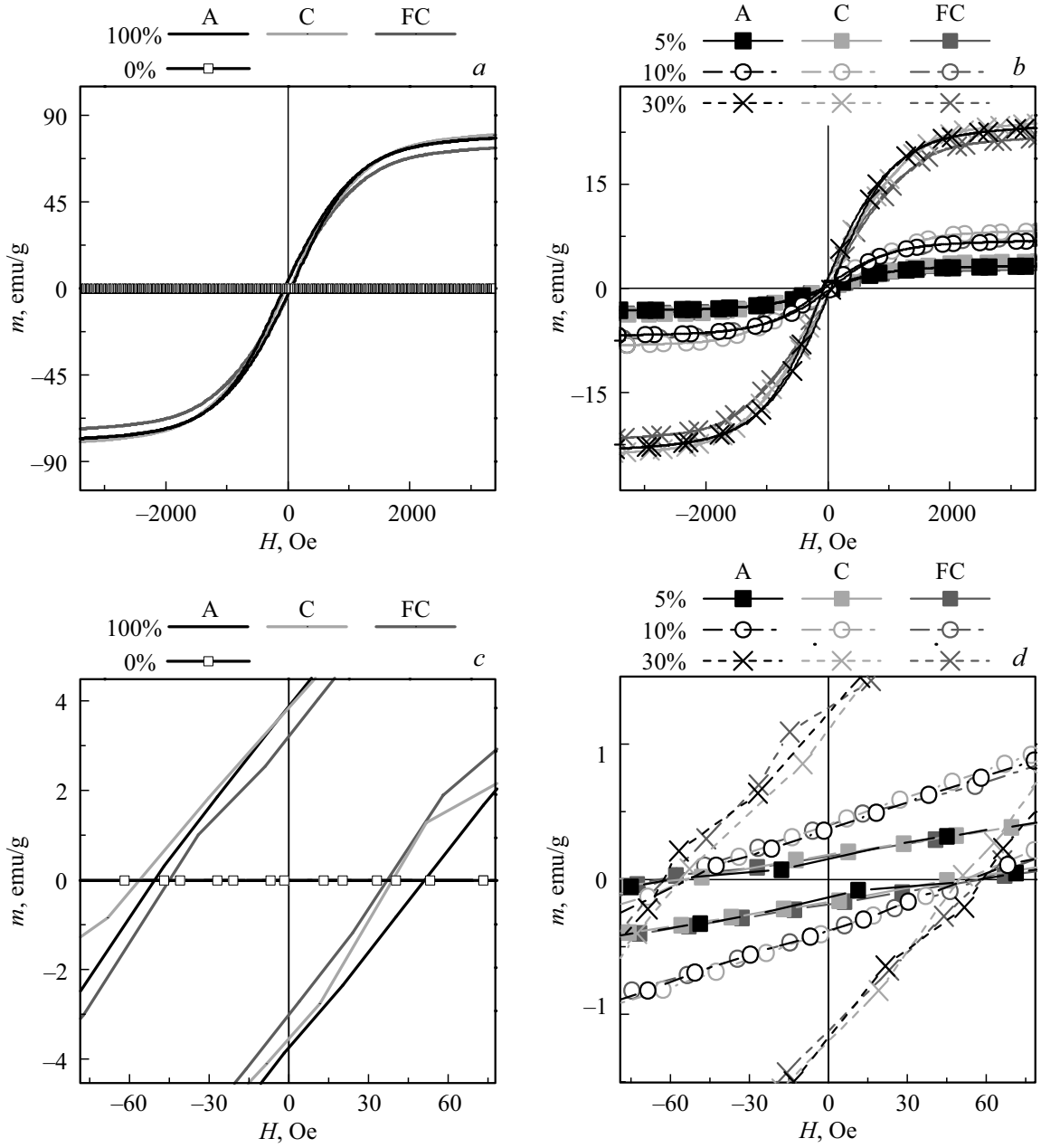

Figure 6. Specific magnetic moment of magnetic particles (a, c) and composites with various weight concentration of particles (b, d): 100% — pure particles, 0% — epoxide resin without particles.

on charts (Fig. 7, a and 8, c), through concentration one may link the values of residual magnetic moment to MI-response, and thus using MI-response value, to determine the residual magnetic moment of composites (Fig. 8, d).

Produced results of comparison of structure features, dispersion parameters, magnetic and MI-properties indicate the possibility of using EWE-nanoparticles with wide size distribution to create model filled composites and applications, which demand large batch size with preservation of the possibility to control dispersion parameters at the expense of changing the process conditions for production of MP.

4. Conclusion

The comparative analysis was carried out on the structure, dispersion parameters and magnetic properties of large batches of magnetic nanoparticles of magnetite produced by electric wire explosion method, and the same parameters defined for commercial microparticles of magnetite. It was established that despite considerable differences in average sizes defined by specific surface, their size parameters defined using X-ray diffraction analysis differ less significantly. In commercial microparticles of magnetite the main phase is Fe_3O_4, and they have the largest average size (around

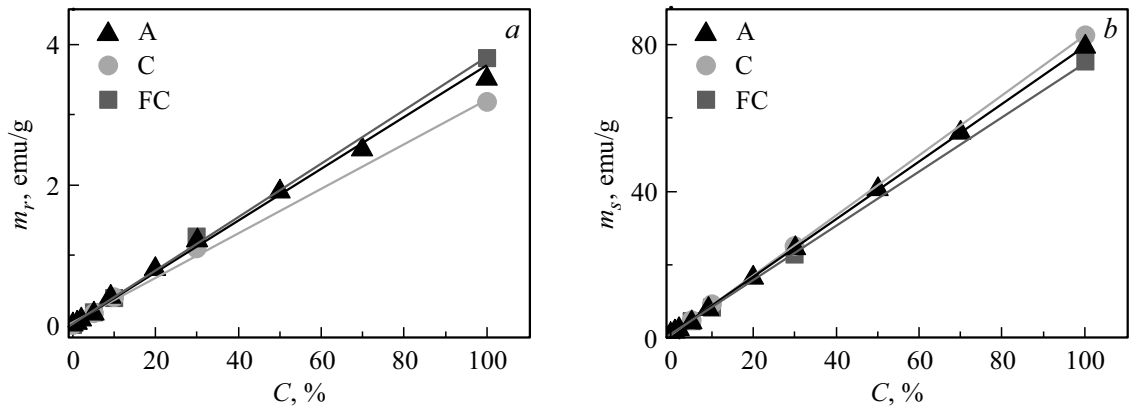

Figure 7. Dependence of specific magnetic moment of particles and composites on their basis on concentration: (*a*) residual magnetic moment, (*b*) magnetic moment of technical saturation (in field of $H = 5$ kOe). Straight — linear approximation by least-square method.

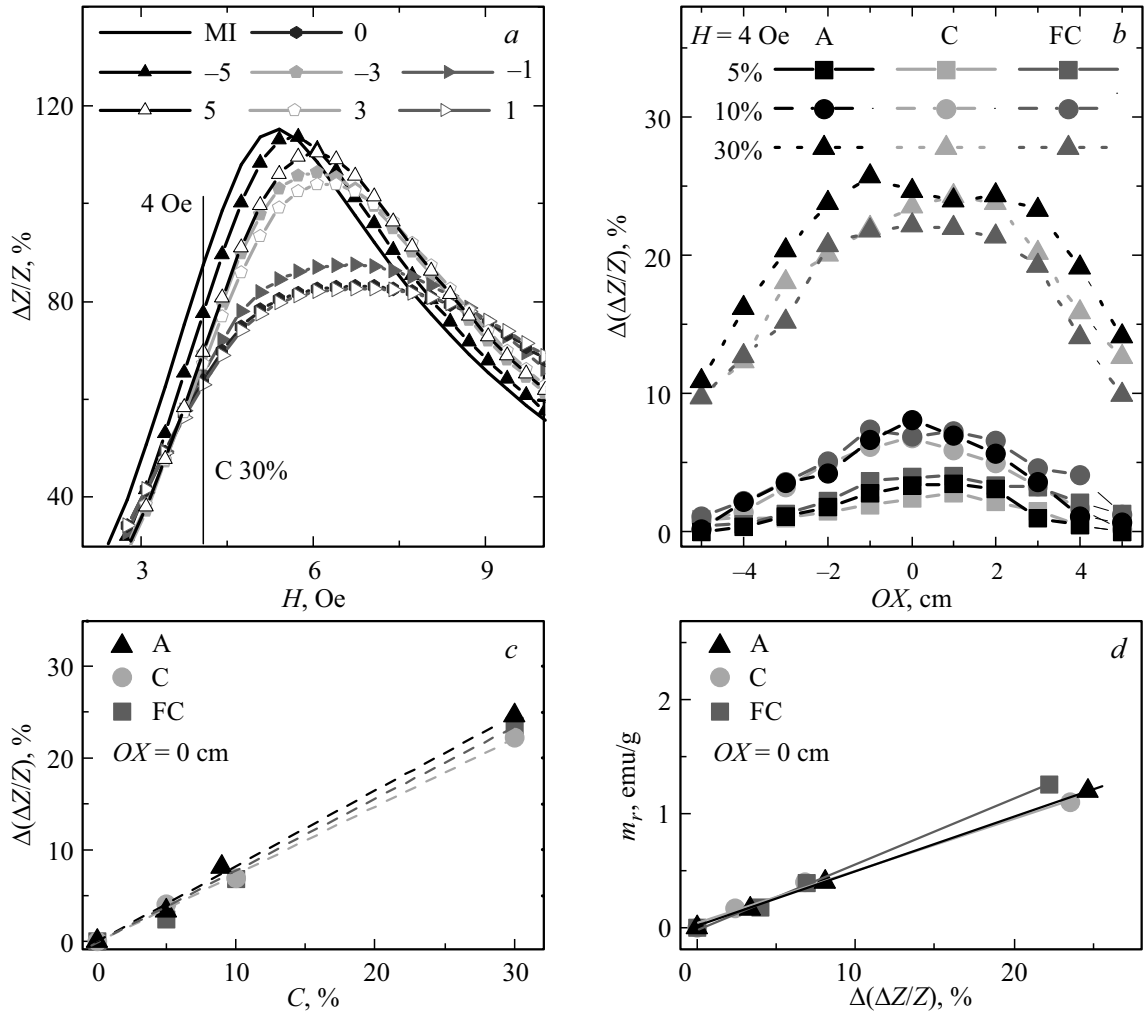

Figure 8. *a*) Field dependence of MI-ratio of the sensitive element at various positions of composite with 30% content of type C particles (figure field shows position of composite in cm; curve „MI“ — MI-ratio of the element without composite). *b*) MI-response of the sensitive element at various positions of composites with various concentration and type of particles, in field $H = 4$ Oe. *c*) Dependence of MI-response on concentration in field $H = 4$ Oe with composite position OX = 0 cm. *d*) Dependence of residual magnetic moment from MI-response calculated by data of fig. 7, *a* and fig. 8, *c*. Straight — linear approximation by least-square method.

240 nm), but their crystal structure is imperfect and contains many defects, and in batches EWE-MP C and FC there are phases Fe_3O_4, Fe_2O_3 and α-Fe, and their crystal structure has higher degree of perfection.

Despite noticeable differences of average sizes and dispersion parameters of micro- and nanoparticles batches, with the matching main magnetic characteristics MI-responses when detecting model samples were close to each other by results of MI-detection with the help of rectangular film MI-element $[FeNi/Cu]_5/Cu/[FeNi/Cu]_5$ in geometry imitating thrombus geometry in a blood vessel. Produced results are important for applications and make it possible to propose detection schemes, for which it is possible to use MP ensembles with wide size distribution.

Acknowledgments

The authors would like to thank A. Larranaga, S. Fernandez-Armas, I. Orue for their collaboration. Certain measurements were carried out in SGIKER services UPV-EHU.

Funding

This study was supported by a grant from the Russian Science Foundation № 23-29-00025, https://rscf.ru/project/23-29-00025/?.

Conflict of interest

The authors declare that they have no conflict of interest.

References

[1] G.I. Frolov, O.I. Bachina, M.M. Zavyalova, S.I. Ravochkin. ZhTF **78**, *8*, 101 (2008) (in Russian).
[2] Q.A. Pankhurst, A.J. Connolly, S.K. Jones, J. Dobson. J. Phys. D **36**, *13*, R167 (2003).
[3] G.V. Kurlyandskaya, A.P. Safronov, S.V. Scherbinin, I.V. Beketov, F.A. Blyakhman, E.B. Makarova, M.A. Korch, A.V. Svalov. FTT **63**, *9*, 1290 (2021). (in Russian).
[4] A.S. Kamzin. FTT **58**, *3*, 519 (2016). (in Russian).
[5] B.M. Geilich, I. Gelfat, S. Sridhar, A.L. van de Ven, T.J. Webster. Biomaterials **119**, 78 (2017).
[6] S.A.M.K. Ansari, E. Ficiara, F.A. Ruffinatti, I. Stura, M. Argenziano, O. Abollino, R. Cavalli, C. Guiot, F. D'Agata. Materials **12**, *3*, 465 (2019).
[7] J.H. Grossman, S.E. McNeil. Phys. Today **65**, 38 (2012).
[8] G.V. Kurlyandskaya, L.S. Litvinova, A.P. Safronov, V.V. Schupletsova, I.S. Tyukova, O.G. Khaziakhmatova, G.B. Slepchenko, K.A. Yurova, E.G. Cherempey, N.A. Kulesh, R. Andrade, I.V. Beketov, I.A. Khlusov, Sensors, **17**, *11*, 2605 (2017).
[9] I.V. Beketov, A.P. Safronov, A.I. Medvedev, J. Alonso, G.V. Kurlyandskaya, S.M. Bhagat. AIP Adv. **2**, 022154 (2012).
[10] Yu.A. Kotov. J. Nanopart. Res. **5**, *5*, 539 (2003).
[11] G.Yu. Melnikov, V.N. Lepalovskij, A.V. Svalov, A.P. Safronov, G.V. Kurlyandskaya. Sensors **21**, 3621 (2021).
[12] A.Y. Prilepskii, A.F. Fakhardo, A.S. Drozdov, V.V. Vinogradov, I.P. Dudanov, A.A. Shtil, P.P. Bel'tyukov, A.M. Shibeko, E.M. Koltsova, D.Y. Nechipurenko. ACS Appl. Mater. Interfaces **10**, 36764 (2018).
[13] L.A. Ramajo, A.A. Cristóbal, P.M. Botta, J.M. Porto López, M.M. Reboredo, M.S. Castro. Compos. Part A Appl. Sci. Manuf. **40**, 388 (2009).
[14] H. Gu, S. Tadakamalla, Y. Huang, H.A. Colorado, Z. Luo, N. Haldolaarachchige, D.P. Young, S. Wei, Z. Guo. ACS Appl. Mater. Interfaces **4**, 5613 (2012).
[15] A. García-Arribas, E. Fernández, A. Svalov, G.V. Kurlyandskaya, J.M. Barandiaran. J. Magn. Magn. Mater. **400**, 321 (2016).
[16] N.A. Buznikov, A.V. Svalov, G.V. Kurlyandskaya. FMM **122**, *3*, 241 (2021). (in Russian).
[17] S.S. Aplesnin, G.I. Barinov, FTT **49**, *10*, 1858 (2007). (in Russian).
[18] G.V. Kurlyandskaya, S.M. Bhagat, A.P. Safronov, I.V. Beketov, A. Larranaga. AIP Adv. **1**, *4*, 042122 (2011).
[19] G.Yu. Melnikov, L.M. Ranero, A.P. Safronov, A. Larranaga, A.V. Svalov, G.V. Kurlyandskaya. FMM **123**, 1145 (2022). (in Russian).

Translated by Ego Translating